

REPORT 1237

A FLIGHT EVALUATION OF THE LONGITUDINAL STABILITY CHARACTERISTICS ASSOCIATED WITH THE PITCH-UP OF A SWEEP-WING AIRPLANE IN MANEUVERING FLIGHT AT TRANSONIC SPEEDS ¹

By SETH B. ANDERSON and RICHARD S. BRAY

SUMMARY

Flight measurements of the longitudinal stability and control characteristics were made on a swept-wing jet aircraft to determine the origin of the pitch-up encountered in maneuvering flight at transonic speeds. For this purpose measurements were made of elevator angle, tail angle of attack, and wing-fuselage pitching moments (obtained from measurements of the balancing tail loads).

The results showed that the pitch-up encountered in a wind-up turn at constant Mach number was caused principally by an unstable break in the wing pitching moment with increasing lift. This unstable break in pitching moment was not present beyond approximately 0.93 Mach number over the lift range covered in these tests. The pitch-up encountered at about 0.95 Mach number in a dive-recovery maneuver was due chiefly to a reduction in the wing-fuselage stability with decreasing Mach number. The severity of the pitch-up was increased by the reduction in elevator effectiveness present at the higher Mach numbers.

INTRODUCTION

The use of swept-wing aircraft has introduced a number of stability and control problems. One problem termed a "pitch-up" has manifested itself essentially in a reversal of the variation of elevator control position and force with normal acceleration. This pitch-up behavior, as far as the pilot is concerned, limits the useful maneuvering range since accelerated flight near the pitch-up region may inadvertently lead to excessive airframe loads or quite rapidly slow the airplane down to the stall.

Previous studies (e. g., ref. 1) have pointed out that the marked increase in nose-up pitching moment of swept wings with increasing lift at the higher lift values and at high subsonic Mach numbers is due to flow separation phenomena near the wing tips. Another factor deemed to be responsible for pitch-up encountered during flight tests on a swept-wing aircraft is an increase in the rate of change of effective downwash at the tail with increase in angle of attack. With regard to the effects of downwash, the results of low-speed tests reported in reference 2 demonstrated that the vertical location of the horizontal tail in the downwash field of a swept wing was the principal factor determining the stability contribution of the horizontal tail; locations above the wing-chord plane extended tended to be destabilizing.

Results of a preliminary flight investigation on the subject airplane (ref. 3) have pointed out the presence of a marked pitch-up in the Mach number range from 0.75 to 0.93. It was mentioned that the following three factors could contribute to the severity of the pitch-up: stick-fixed longitudinal instability at high lift coefficients, an increase in elevator effectiveness with decreasing Mach number, and a reduction in longitudinal stability with decreasing Mach number.

Flight-test results presented herein serve to extend the scope of the results of reference 3 and point out the causes of the pitch-up and the degree to which the various factors involved contribute to the overall behavior of the airplane.

INTRODUCTION

A_z	ratio of net aerodynamic force along airplane z axis to the weight of the airplane, positive when directed upward (A_z of 1 = 1 g)
b	wing span, ft
c	wing chord (parallel to plane of symmetry), ft
\bar{c}	mean aerodynamic chord, $\frac{\int_0^{b/2} c^2 dy}{\int_0^{b/2} c dy}$, ft
C_m	pitching-moment coefficient of airplane about 0.25 M.A.C.
C_{m_w}	pitching-moment coefficient of wing about 0.25 M.A.C.
$C_{m_{w+f}}$	pitching-moment coefficient of wing-fuselage combination about 0.25 M.A.C.
$\frac{\partial C_m}{\partial \alpha}$	rate of change of airplane pitching-moment coefficient with angle of attack, per deg
$\frac{\partial C_m}{\partial C_N}$	rate of change of airplane pitching-moment coefficient with normal-force coefficient
$\frac{\partial C_m}{\partial \delta_e}$	elevator effectiveness parameter, per deg
$\left(\frac{\partial C_m}{\partial C_N}\right)_t$	rate of change of pitching-moment coefficient due to the horizontal tail with normal-force coefficient
$\frac{\partial C_m}{\partial i_s}$	stabilizer effectiveness parameter, per deg

¹ Supersedes NACA RM A51112 by Seth B. Anderson and Richard S. Bray, 1951.

C_N	airplane normal-force coefficient, $\frac{WA_z}{qS}$
c_n	wing-section normal-force coefficient
$\frac{\partial C_N}{\partial \delta_e}$	rate of change of airplane normal-force coefficient with elevator deflection, per deg
$\frac{\partial C_N}{\partial \alpha}$	lift-curve-slope parameter
F_e	elevator control force, lb
i_s	stabilizer setting (positive, leading edge up), deg
L_t	horizontal-tail load (positive upwards), lb
M	free-stream Mach number
q	free-stream dynamic pressure, lb/sq ft
q_t	ratio of dynamic pressure at horizontal tail to free-stream dynamic pressure
R	Reynolds number based on wing M.A.C.
S	wing area, sq ft
W	airplane weight, lb
y	spanwise distance from plane of symmetry, ft
α	airplane angle of attack, deg
α_t	tail angle of attack, deg
ϵ	downwash angle, deg
$\frac{\partial \epsilon}{\partial C_N}$	downwash parameter
δ_e	elevator angle (with respect to stabilizer), deg
δ_a	aileron angle, deg
$\frac{\Delta i_s}{\Delta \delta_e}$	relative elevator-stabilizer effectiveness
SUBSCRIPTS	
i	inboard
o	outboard

AIRPLANE DESCRIPTION

The test airplane was a jet-powered fighter type having sweptback wing and tail surfaces. A photograph of the airplane is presented in figure 1 and a two-view drawing of the airplane is given in figure 2. A description of the geometric details of the airplane is given in table I. It should be noted that the test airplane was not equipped with an elevator bungee or bob weight.



FIGURE 1.—Photograph of the test airplane.

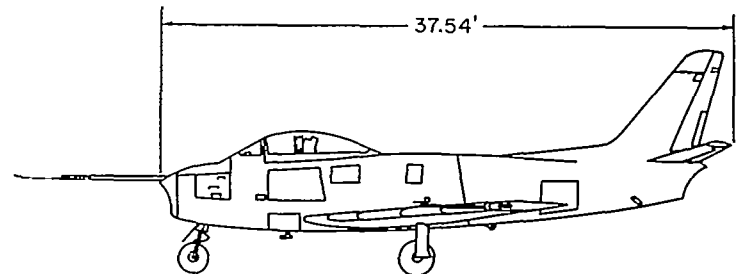
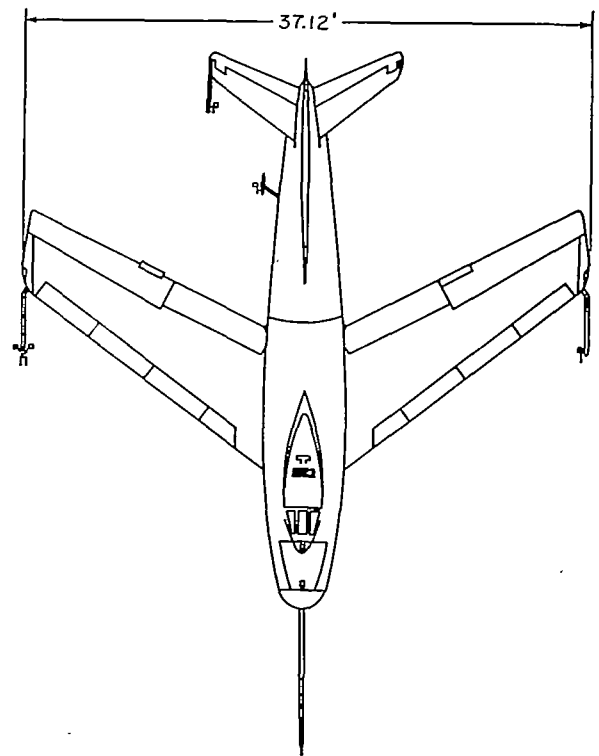


FIGURE 2.—Two-view drawing of test airplane showing research airspeed installation.

INSTRUMENTATION

Standard NACA instruments and an 18-channel oscillograph were used to record values of airspeed, altitude, acceleration, elevator control force, and positions of the elevator, horizontal stabilizer, and ailerons. Tail dynamic-pressure measurements were made at 92 percent of the tail semispan. Horizontal-tail loads were measured by means of strain gages at the three pin-joined fittings where the tail is joined to the fuselage. Wing pressure-distribution measurements were made on a companion airplane by means of absolute pressure transmitters.

Airplane angle of attack was measured by a vane mounted on a boom one tip-chord length ahead of the wing tip. Tail angle-of-attack measurements used in the pitch-up analysis were obtained by a vane on a boom one and one-half tip chord lengths ahead of the horizontal-tail tip. An additional tail angle-of-attack measurement was made by a fuselage boom in order to obtain tail angle-of-attack values at two spanwise stations (22- and 92-percent tail semispan).

TABLE I.—DESCRIPTION OF TEST AIRPLANE

Wing:	
Total wing area (including flaps, slats, and 49.92 sq ft covered by fuselage).....	287.90 sq ft
Span.....	37.12 ft
Aspect ratio.....	4.79
Taper ratio.....	0.51
Mean aerodynamic chord (wing station 98.7 in.)..	8.08 ft
Dihedral angle.....	3.0°
Sweepback of 0.25-chord line.....	35°14'
Sweepback of leading edge.....	37°44'
Aerodynamic and geometric twist.....	2.0°
Root airfoil section (normal to 0.25-chord line)	NACA 0012-64 (modified)
Tip airfoil section (normal to 0.25-chord line)	NACA 0011-64 (modified)
Ailerons	
Total area.....	37.20 sq ft
Span.....	9.18 ft
Chord (average).....	2.03 ft
Horizontal tail:	
Total area (including 1.20 sq ft covered by vertical tail).....	34.99 sq ft
Span.....	12.75 ft
Aspect ratio.....	4.65
Taper ratio.....	0.45
Dihedral angle.....	10.0°
Root chord (horizontal-tail station 0).....	3.79 ft
Tip chord (equivalent horizontal-tail station 76.68 in.).....	1.74 ft
Mean aerodynamic chord (horizontal-tail station 33.54 in.).....	2.89 ft
Sweepback of 0.25-chord line.....	34°35'
Airfoil section (parallel to center line).....	NACA 0010-64
Maximum stabilizer deflection.....	+1° up, -10° down
Elevator:	
Area (including tabs and excluding balance area forward of hinge line).....	10.13 sq ft
Span, each.....	5.77 ft
Chord, inboard (equivalent horizontal-tail station 6.92 in.).....	1.19 ft
Chord, outboard (theoretical horizontal-tail station 76.18 in.).....	0.57 ft
Maximum elevator deflection.....	35° up, 17.5° down
Boost.....	hydraulic

The angle of attack values were corrected for induced flow effects at the tip booms. Elevator, horizontal stabilizer, and aileron position angles were measured in planes normal to the hinge lines.

Values of Mach number were obtained using the nose boom airspeed system described in reference 4.

TEST PROCEDURE

Tests were conducted over a Mach number range extending from 0.8 to 1.03 and through an altitude range from 40,000 to 30,000 feet. Below a Mach number of 0.93, data were obtained in steady 1 g flight and in steady turns at constant Mach number up to those values of normal-force coefficient where the pitch-up was encountered. At this point the controls were held steady, allowing the airplane to pitch up to the stall or the limit acceleration factor. Data, corrected for pitching acceleration effects, were used from portions

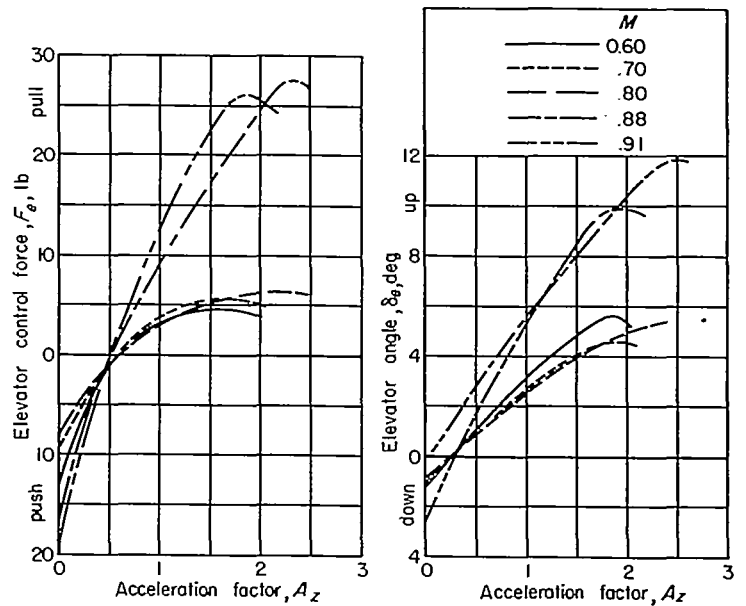


FIGURE 3.—Variation of elevator angle and force with normal acceleration for several Mach numbers.

of these records which showed no significant Mach number variations. Between 0.93 and 0.96 Mach number only a limited C_N range (0.05 to 0.40) was covered, due to low elevator effectiveness and the difficulty of maintaining steady wings-level flight in this region. Above 0.96 Mach number a larger C_N range was covered by use of the movable stabilizer as the primary longitudinal control (elevator held fixed).

The tests were conducted with the center of gravity at an average value of 0.225 M. A. C. and a gross weight of 12,750 pounds. Except where otherwise stated, a stabilizer incidence setting of 0.6° was used. The automatic leading-edge slats remained retracted over the range of tests presented in this report.

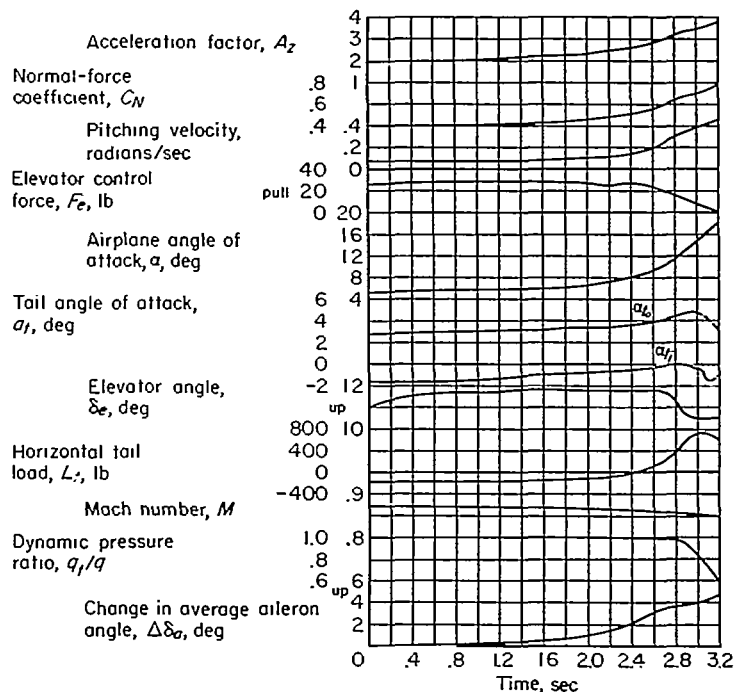


FIGURE 4.—Time-history plot of a pitch-up encountered in a wind-up turn.

Data from tests of a semispan 0.20-scale model of the airplane in the Ames 16-foot high-speed wind tunnel were used to compare flight and wind-tunnel results in various parts of the report.

RESULTS AND DISCUSSION

Previous operation of the test airplane (ref. 3) disclosed the presence of a pitch-up during maneuvering flight at constant Mach number in the Mach number range from 0.75 to 0.93. In addition it was noted that a pitch-up would occur in recovering from a high-speed dive when slowing down through 0.95 Mach number.

In order to point out more clearly the reasons for the pitch-up behavior of the test airplane, the discussion and analysis of the data have been divided into a part covering the case at varying lift and constant Mach number such as occurs in a wind-up turn, and at varying Mach number and essentially constant lift coefficient as in a high-speed pull-out maneuver. In addition, other items not directly connected with the pitch-up analysis, but serving to document the longitudinal stability and control characteristics of the airplane, are discussed in Appendix A.

PITCH-UP CHARACTERISTICS AT CONSTANT MACH NUMBER

The pitch-up characteristic of the airplane is illustrated by the stick-fixed and stick-free longitudinal data in figure 3 and the time-history plot of a wind-up turn in figure 4. The drop-off in elevator control force and deflection at the higher A_z values is shown by the data in figure 3. The portion of the time-history plot (fig. 4), taken at a Mach number (0.87), for which the pilot noted the pitch-up to be relatively abrupt, shows that after approximately 1.5 seconds the normal acceleration continued to increase despite the fact that no additional up-elevator deflection or pull force was applied. It can be noted that during the pitch-up an increasing upload was measured at the horizontal tail, thereby indicating that the source of the pitch-up was not at the tail itself. The time-history results plotted in more complete form against C_N (fig. 5) show the manner in which the various factors vary with C_N . It can be seen that the elevator angle and control-force variations were nonlinear beyond $C_N=0.4$.

The reason for the pitch-up can be deduced from an examination of the action of the factors governing the longitudinal control of the airplane; namely, the pitching moments due to the wing-fuselage combination and those due to the horizontal tail. This is demonstrated in figure 6 which shows the computed increment in δ_e required to balance the changes with C_N of the wing-fuselage pitching moment (obtained from the tail-load measurements) and that due to the change in tail angle of attack. Comparison of these values with the measured flight values of δ_e shows that a reduction

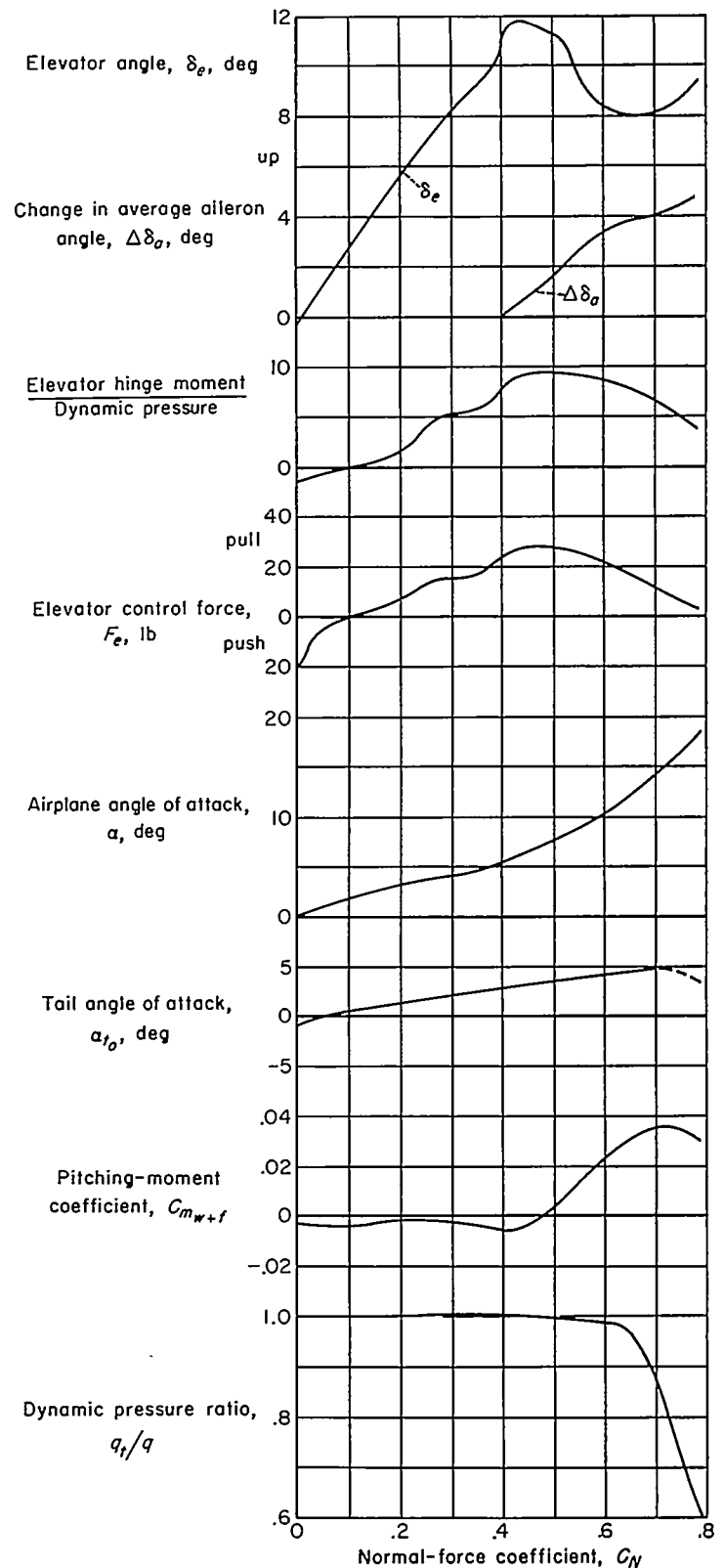


FIGURE 5.—Variation of the longitudinal control characteristics with normal-force coefficient; Mach number=0.87.

* The method for calculating the elevator angles used in figure 6 is given in Appendix B.

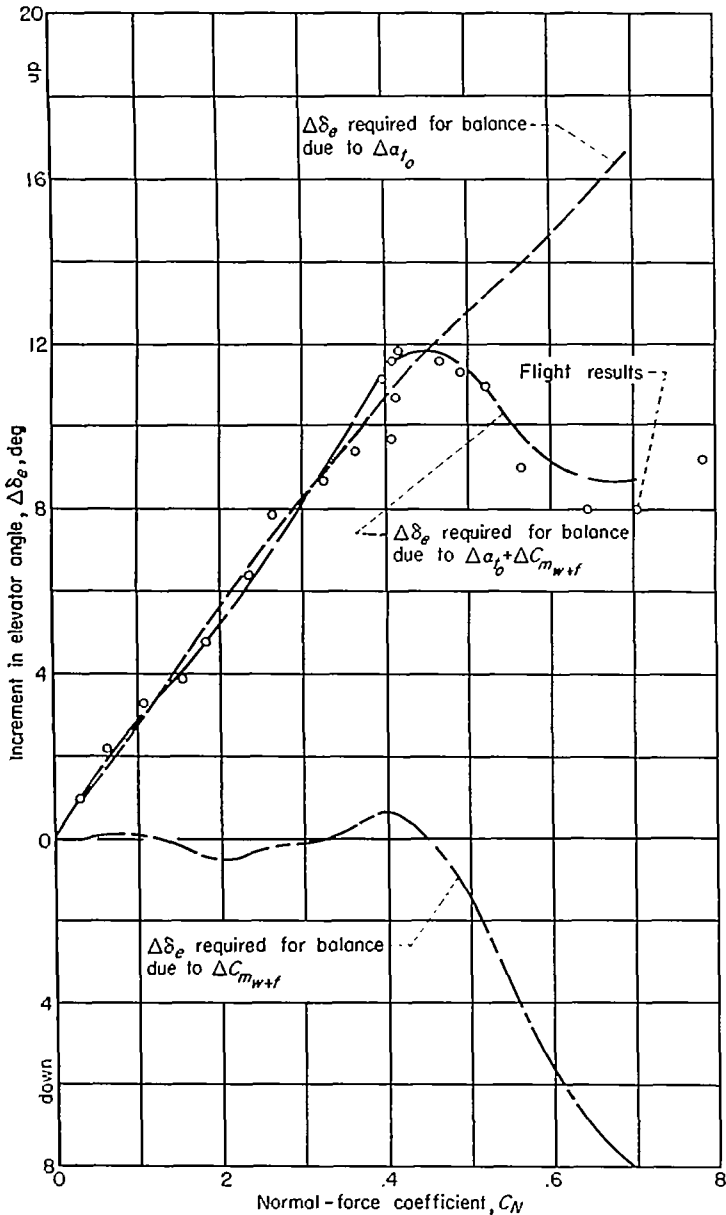


FIGURE 6.—Variation with C_N of elevator angle required for balance; Mach number=0.87.

in elevator deflection with increasing lift beyond $C_N=0.4$ is required to balance the action of the wing-fuselage pitching moment. The horizontal-tail contribution is shown to be stabilizing over the entire C_N range.

The reason for the variation in the wing-fuselage pitching moment noted previously has been traced to the lift characteristics of the wing itself by means of pressure-distribution measurements. Figure 7 presents data showing a comparison between the wing-fuselage pitching moments derived from the tail-load measurements and the wing pitching moments obtained from the wing-panel loadings. These results indicate that the change in pitching moment at the higher C_N values is accounted for principally by the wing contribution.

The change in wing pitching moment with increase in C_N is the result of a redistribution of lift carried by the wing, comprised of a spanwise and chordwise loading shift. The relative magnitudes of the chordwise and spanwise load changes are compared in figure 8 in terms of pitching-moment

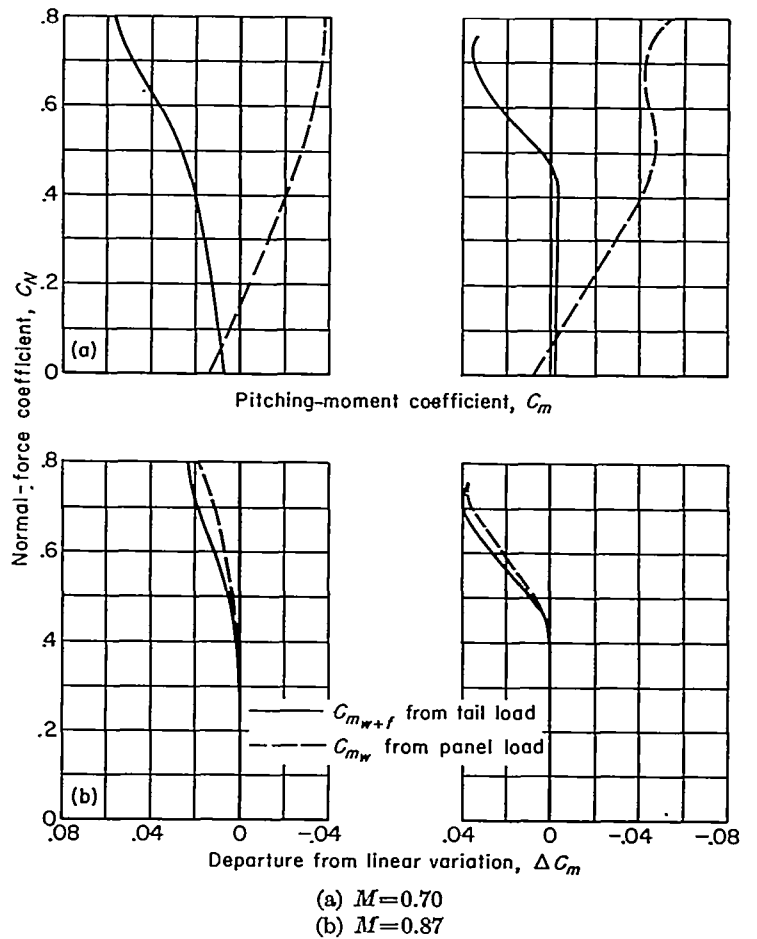


FIGURE 7.—Variation of C_m with C_N as obtained from tail load measurements and wing panel load measurements.

variation with C_N . These results show that the chordwise shift produces a stable pitching-moment variation, while the spanwise shift is the factor responsible for the destabilizing action of the wing. This destabilizing pitching-moment variation is due to an inboard shift in loading at the higher lift values. The section C_N data of figure 9 show that this results from a reduction in lift near the wing tips which, in turn, is believed to result from shock-induced separation effects. Additional evidence of separation is given by the fact that the break in the pitching-moment curves corresponds to the onset of buffeting. Thus, for various Mach

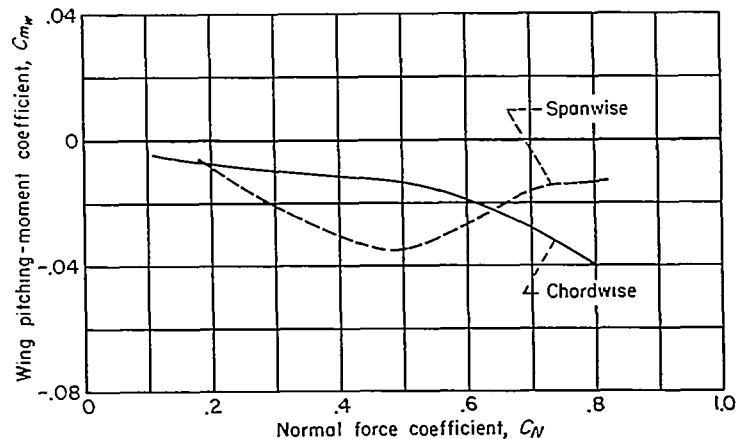


FIGURE 8.—Variation of wing pitching-moment coefficient with airplane normal-force coefficient due to changes in chordwise and spanwise loadings; Mach number=0.87.

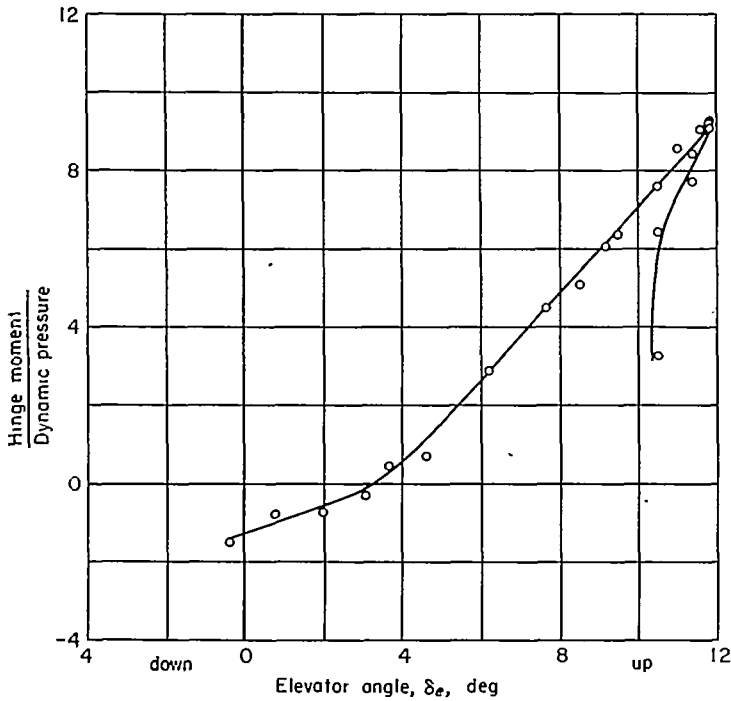


FIGURE 11.—Variation of elevator hinge moment with deflection for wind-up turn; Mach number=0.87.

deflection, at which point the pitch-up occurred. Beyond this point, as the normal acceleration increased in the pitch-up, the hinge moment fell off rapidly with the reduction in elevator angle, thereby tending to increase the severity of the pitch-up apparent to the pilot.

PITCH-UP CHARACTERISTICS AT VARYING MACH NUMBER

A time-history plot illustrating a pitch-up which occurred at a particular Mach number when slowing down from a high-speed dive is presented in figure 12. These data show that at 5.5 seconds (0.95 Mach number) the normal acceleration and pitching velocity continued to increase despite the fact that the elevator deflection was decreased.

The cause of this pitch-up with decreasing Mach number may be determined by an inspection of the pitching moments arising from the change in the horizontal-tail angle of attack and of the wing-fuselage pitching moments. In this regard, the data in figure 13 show the variation with Mach number of angle of attack at the tail and wing-fuselage pitching moment for various constant values of normal-force coefficient from 0 to 0.7. For the C_N value (of the order of 0.4) for the pull-out time-history illustration, the data in figure 13 show that in slowing down in the region of 0.95 Mach number the tail experienced an increase in angle of attack, thus promoting a diving tendency, while the wing-fuselage pitching-moment coefficient varied in a direction to produce the pitch-up. The magnitude of the change in pitching moment over a given Mach number range was greater the higher the C_N value, thereby making pull-outs initiated at high C_N values more critical.³

The change in pitching moment, which is responsible for the pitch-up when decreasing Mach number, is chiefly the result of a stability change of the wing-fuselage combination.

³ In normal operation of the test airplane, increases in speed are necessarily made in dives at low C_N values, whereas recoveries are executed at high C_N values.

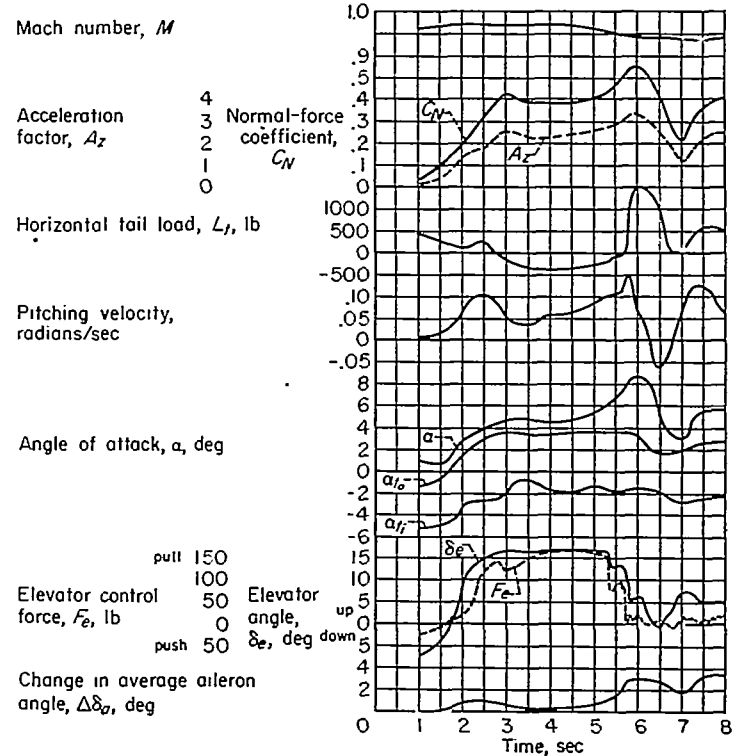


FIGURE 12.—Time-history plot of a pull-out in which a pitch-up occurred as the Mach number decreased.

This is shown in figure 10 by the rotation of the C_m-C_N curves indicating a change from a stabilizing to a destabilizing condition when decreasing Mach number in the range from 1.0 to 0.85. Wing pressure-distribution measurements not presented herein indicate that at the higher C_N values the resultant nose-up pitching moment is due to a forward longitudinal shift in the center of pressure with decreasing Mach number. For these same conditions the location of the center of pressure moved outboard.

The effect of a change in elevator effectiveness with Mach number is an important item in judging the longitudinal behavior of the airplane so far as the pilot is concerned. The reduction in elevator effectiveness beyond 0.8 Mach number shown in figure 13 is reflected by the large variation of elevator angle required for balance in the Mach number range above 0.85 Mach number. The amount of additional elevator angle needed for balance because of the reduced effectiveness is brought out in figure 14 by comparing the measured values of δ_e with those calculated assuming a constant control effectiveness (value at $M=0.6$) over the test Mach number range for $C_N=0.3$. The reduction in elevator effectiveness beyond 0.9 Mach number greatly restricts the use of the elevator control for maneuvering, the stabilizer becoming the preferred control. It should be emphasized that the change in elevator effectiveness is not the cause of the pitch-up, but it does serve to accentuate the pitch-up.

SUMMARY OF RESULTS

Results of flight tests conducted on a swept-wing, fighter-type jet aircraft to investigate the longitudinal-stability and control characteristics associated with a pitch-up showed the following:

1. The pitch-up encountered in a wind-up turn at constant

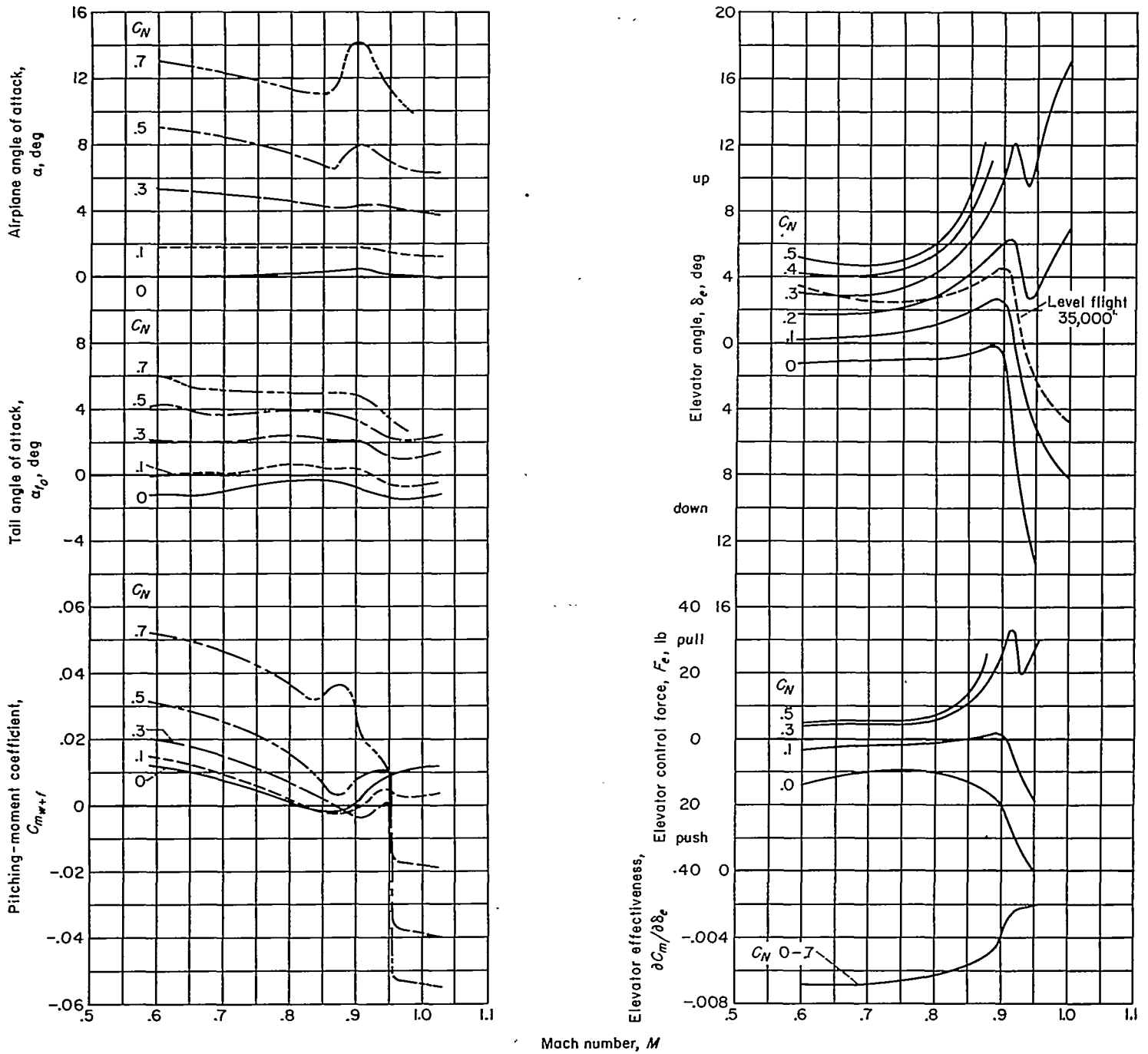


FIGURE 13.—Variation of the longitudinal-control characteristics with Mach number.

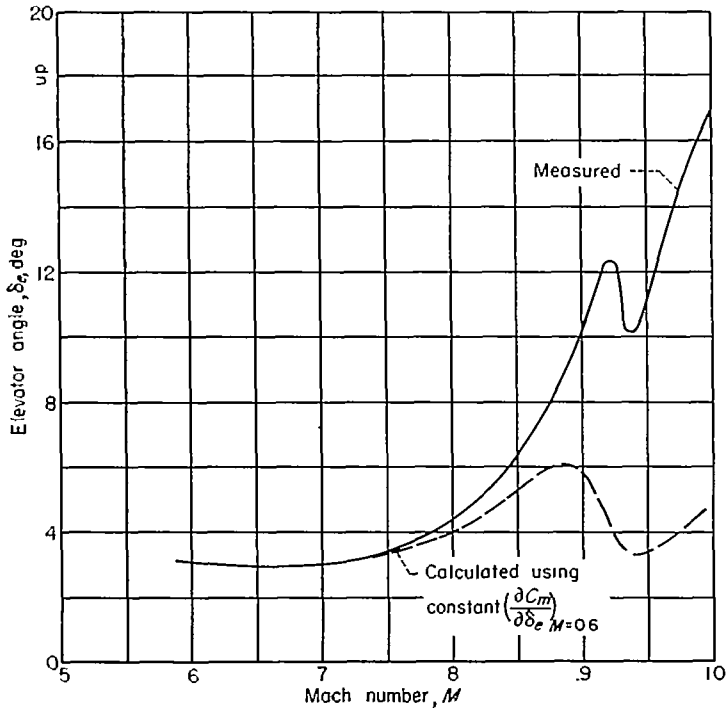


FIGURE 14.—Variation with Mach number of elevator angle required for balance at $C_N=0.3$.

Mach number was caused principally by an unstable break in the wing pitching moment which, in turn, was caused by a reduction of lift near the wing tips.

2. The unstable break in the measured wing-fuselage pitching-moment curves was more abrupt in the Mach number range from 0.83 to 0.91, the instability tending to disappear at the higher C_N values. No instability was measured for the lift range covered for Mach numbers in excess of about 0.93.

3. The pitch-up encountered in a dive recovery at 0.95 Mach number was caused chiefly by a reduction in the wing-fuselage stability with decreasing Mach number resulting from a forward chordwise shift in loading of the wing.

4. At high Mach numbers the elevator was unsatisfactory for longitudinal control. The reduction in elevator effectiveness at speeds beyond 0.90 Mach number accentuated the pitch-up and restricted the maneuverability, which resulted in the stabilizer becoming the preferred longitudinal control.

AMES AERONAUTICAL LABORATORY,
 NATIONAL ADVISORY COMMITTEE FOR AERONAUTICS,
 MOFFETT FIELD, CALIF., Sept. 12, 1951.

APPENDIX A

ADDITIONAL LONGITUDINAL-STABILITY AND -CONTROL CHARACTERISTICS

In the following paragraphs a number of items documenting the longitudinal-stability and -control characteristics over the test Mach number range are discussed.

The variation with Mach number of a number of aerodynamic parameters compared favorably with wind-tunnel results taken over the C_N range for steady flight conditions at 1 g (fig. 15). Discrepancies which do exist may result

from Reynolds number differences for the two results (Reynolds number ranges shown in fig. 16). The results in figure 15 show an increase in airplane stability, $\partial C_m / \partial C_N$, with increase in Mach number amounting to a 12.5-percent rearward shift in the aerodynamic center. The increase in airplane stability beyond 0.85 Mach number is shown to be due to the increased stability of the wing-fuselage combination. The tail contribution to the stability $(\partial C_m / \partial C_N)_t$ showed a decrease beyond 0.90 Mach number following the increase in the downwash factor $\partial \epsilon / \partial C_N$ at the same Mach number. The airplane lift-curve slope $\partial C_N / \partial \alpha$ is shown to increase steadily up to about 0.89 Mach number and then drops off slightly to the highest test Mach number.

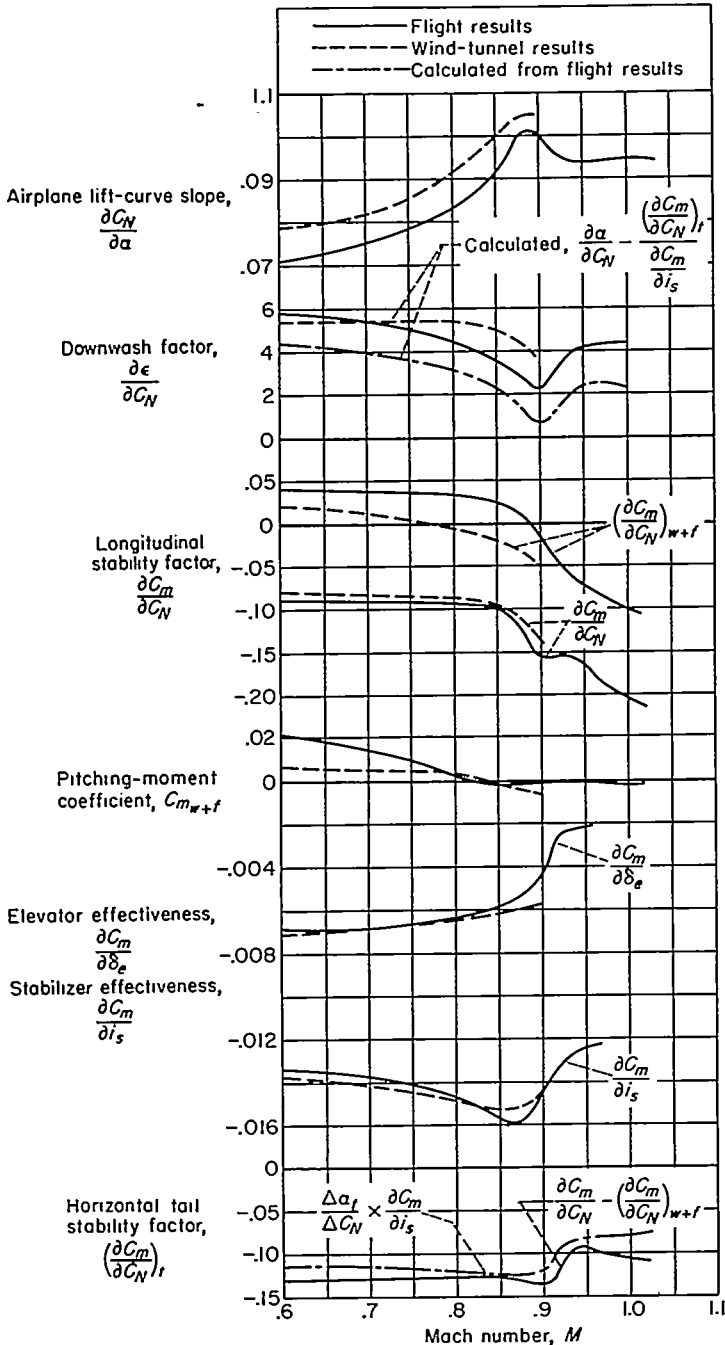


FIGURE 15.—Variation with Mach number of a number of aerodynamic parameters and a comparison with wind tunnel results; steady level flight.

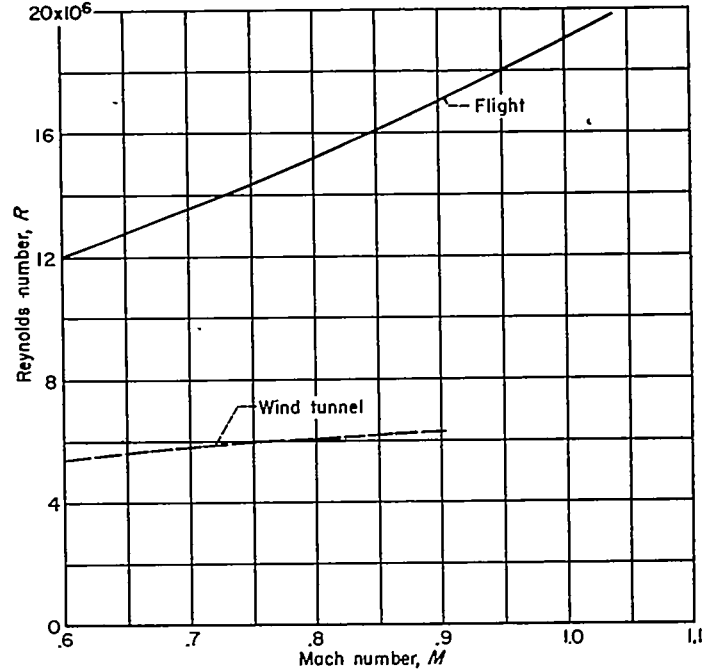


FIGURE 16.—Variation of average Reynolds number with Mach number.

The wing-fuselage pitching-moment coefficient decreased steadily from a positive value at low Mach numbers to a negative value at about 0.85 Mach number, and then remained essentially constant to the highest test Mach number. It should be noted that the wing-fuselage pitching-moment values presented in figure 15 (and in fig. 13 for various C_N values) were obtained from horizontal tail-load measurements. In this regard the $C_{m_{w+f}}$ values indicate indirectly the balancing tail loads over a wide range of normal-force coefficient and Mach number. These data indicate an increase in down load with increase in Mach number through 0.95 for C_N values in excess of approximately 0.2.

The variation of the elevator effectiveness $\partial C_m / \partial \delta_e$ and stabilizer effectiveness $\partial C_m / \partial i_s$ over the Mach number range

is given in figure 15. These results indicate that at the highest test Mach number $\partial C_m/\partial \delta_e$ was reduced to 30 percent of its low Mach number value, while $\partial C_m/\partial i_s$ was reduced only 10 percent.

The elevator angle required for balance over the Mach number range for steady flight at 1 *g* and for various constant values of normal-force coefficient have been presented in figure 13. With increasing Mach number (for the higher C_N values), these data indicate an increased diving tendency below 0.9 Mach number and a decreased climbing tendency beyond 0.9 Mach number. These effects are caused primarily by changes in the pitching moments arising from the wing-fuselage and the change in angle of attack at the tail.

The elevator control power, illustrated by the data in figure 3, indicates an increase in elevator-control gradient and force gradient with an increase in Mach number above 0.80 for values near $A_z=1$. The power of the elevator is illustrated further in figure 17 in the variation of $\partial C_N/\partial \delta_e$ (linear C_N region) with Mach number for the measured

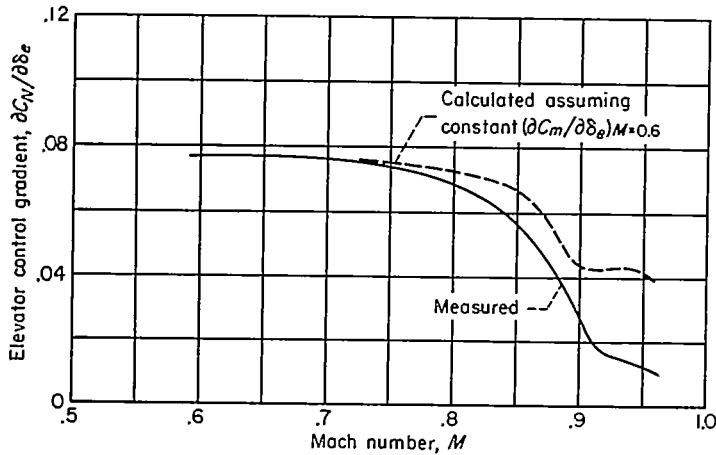


FIGURE 17.—Variation with Mach number of the elevator control gradient.

values and for values calculated assuming no reduction in elevator effectiveness ($\partial C_m/\partial \delta_e$ held constant at the value for $M=0.6$). These results show that approximately 50 percent of the change in $\partial C_N/\partial \delta_e$ from the value at low speed to that at the highest Mach number can be attributed to a reduction in elevator effectiveness and the remainder to an increase in airplane stability.

The effect of a change in stabilizer setting on the elevator angle required for steady 1 *g* flight is shown by the data in figure 18. These results indicate an increase in the diving tendency with a positive increase in stabilizer incidence below 0.9 Mach number. Beyond 0.9 Mach number a climbing tendency is indicated for all stabilizer settings. The Mach number range for these data was limited due to the effect of the reduced elevator effectiveness and the large control

forces associated with the out-of-trim stabilizer settings used. Cross plots of the data of figure 18 show a marked decrease in the relative elevator-stabilizer effectiveness (fig. 19) beyond 0.7 Mach number.

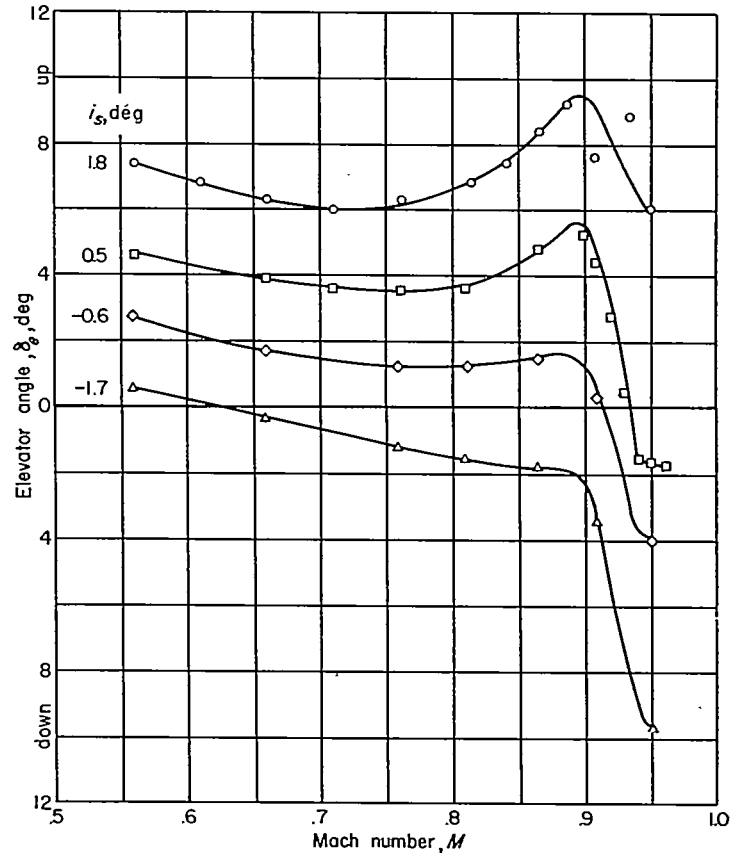


FIGURE 18.—Variation with Mach number of elevator angle required for steady level flight for various stabilizer settings.

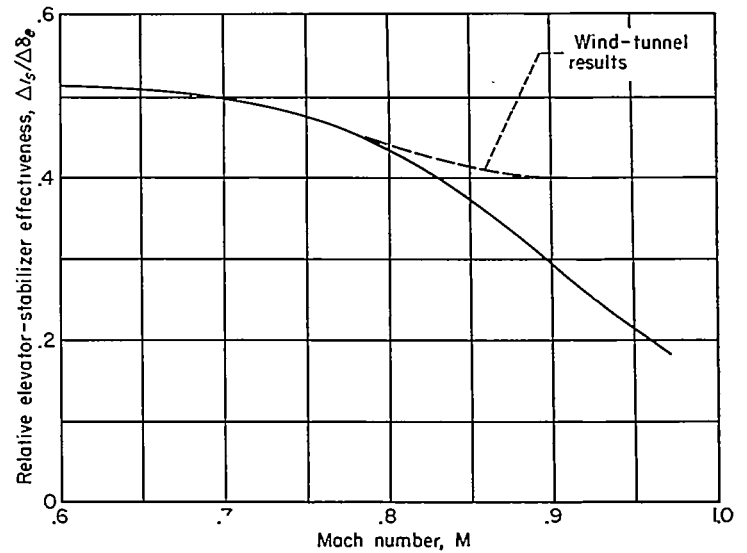


FIGURE 19.—Variation with Mach number of relative elevator-stabilizer effectiveness parameter.

APPENDIX B

ELEVATOR-ANGLE CALCULATIONS

The computed changes in elevator angle used in figure 6 were determined from

$$\Delta\delta_e = \frac{\Delta C_{m_{w+f}} + \frac{\partial C_m}{\partial i_z} \Delta\alpha_{t_0}}{\frac{\partial C_m}{\partial \delta_e}}$$

where $C_{m_{w+f}}$ was obtained from tail-load measurements; and $\frac{\partial C_m}{\partial i_z}$, from $\frac{\partial C_m}{\partial \delta_e} \frac{\Delta\delta_e}{\Delta i_z}$ where $\frac{\Delta\delta_e}{\Delta i_z}$ is the relative elevator-stabilizer effectiveness shown in figure 19; and $\frac{\partial C_m}{\partial \delta_e}$ is obtained from

$$\frac{\partial C_m}{\partial \delta_e} = - \left(\frac{\partial C_m}{\partial \alpha} \frac{\partial \alpha}{\partial C_N} \frac{\partial C_N}{\partial \delta_e} \right)$$

where $\frac{\partial C_m}{\partial \alpha}$ was obtained from reference 5 which used the pulse-response technique. These data were obtained only over a limited C_N range (that for steady flight at $A_z=1$); however, results from unpublished wind-tunnel tests on a model of the test airplane indicate constant $\frac{\partial C_m}{\partial \delta_e}$ values over

the C_N range covered in these tests. Values of $\frac{\partial C_N}{\partial \alpha}$ and $\frac{\partial C_N}{\partial \delta_e}$ were obtained from flight-test measurements.

REFERENCES

1. Gøthert, B.: High-Speed Measurements on a Swept-Back Wing (Sweepback Angle $\varphi=35^\circ$). NACA TM 1102, 1947.
2. Furlong, G. Chester, and Bollech, Thomas V.: Downwash, Sidewash, and Wake Surveys Behind a 42° Sweptback Wing at Reynolds Number of 6.8×10^6 with and without a Simulated Ground. NACA RM L8G22, 1948.
3. Rathert, George A., Jr., Ziff, Howard L., and Cooper, George E.: Preliminary Flight Investigation of the Maneuvering Accelerations and Buffet Boundary of a 35° Swept-Wing Airplane at High Altitude and Transonic Speeds. NACA RM A50L04, 1951.
4. Thompson, Jim Rogers, Bray, Richard S., and Cooper, George E.: Flight Calibration of Four Airspeed Systems on a Swept-Wing Airplane at Mach Numbers Up to 1.04 by the NACA-Radar-Phototheodolite Method. NACA RM A50H24, 1950.
5. Triplett, William C., and Van Dyke, Rudolph D., Jr.: Preliminary Flight Investigation of the Dynamic Longitudinal-Stability Characteristics of a 35° Swept-Wing Airplane. NACA RM A50J00a, 1950.